

# Comparative Analysis of Bi-Static GPR Calibration Techniques

Rohit Kumar Karnena  
*Electronics and Communication  
 Engineering  
 NIT Rourkela  
 India  
 517ec1007@nitrkl.ac.in*

Subrata Maiti  
*Electronics and Communication  
 Engineering  
 NIT Rourkela  
 India  
 smaiti@nitrkl.ac.in*

**Abstract**— Ground penetrating radar (GPR) is a promising non-destructive sensors for subsurface investigation. Calibration of GPR system plays an important role to compensate antenna effect and frequency dependent delay. In this work, two different approaches for SFCW GPR calibration have been studied. A simplified analytical full wave model (FWM) is used as a forward model and copper plate is used as a target. Both the approaches have been validated with laboratory experiments. The comparison of the two approaches has been presented. These calibration approaches are useful for investigating the subsurface media properties, imaging and detection of buried target.

**Keywords**— SFCW GPR, Bi-static, LTF, Calibration, FWM

## I. INTRODUCTION

There has been an increase in demand of GPR for subsurface investigation because of its ability to detect both metallic and non-metallic targets. Stepped frequency continuous wave (SFCW) GPR provides certain advantages like better SNR, efficient calibration than impulse GPR. Antenna, which is a crucial block in GPR system, provides significant distortion in GPR data. Antenna-medium interaction also results in undesired reflections. These inaccuracies caused during GPR measurements need to be removed before GPR data processing. A suitable calibration method can be used for this.

A novel free space calibration method has developed by Mansor Nakhkash et al. [3]. A commercial monostatic GPR is used for investigation of permittivity and conductivity of materials. Antenna-medium coupling has considered in calibration. The developed method has validated with computer simulated and experimental data for concrete block and plain slab. The proposed method consider monostatic GPR. Valeri A Micknev et al [4], has proposed a modified procedure for SFCW GPR calibration. The unwanted reflections from clutters have efficiently removed by using the procedure. Shallow subsurface objects has discriminated and detected using the proposed calibration method. Adaptive software gating calibration method [5] is presented to remove the antenna delay and clutters in GPR antenna footprint measurement. Significant improvement in footprint measurement has observed after calibration. Archimedean spirals are considered for footprint measurement. But, the measured footprint patterns are sensitive to lower frequencies which results inaccuracy in pattern below 1800 MHz. Lambot et al. has proposed a Linear Transfer Function (LTF) method [6] to calibrate off-ground monostatic GPR. A perfectly electrical conducting (PEC) plate is considered as known target. Antenna is calibrated by taking measurements for

multiple antenna-PEC distances. The forward model used in proposed LTF method is conventional FWM which is computationally inefficient. The proposed calibration method is applied for monostatic GPR but not applied for bi-static GPR. Average removal calibration and LTF calibration methods for SFCW GPR has presented Shwetha et al [7]. The comparative analysis of these two methods for off ground monostatic GPR has given. LTF method gives better results than average removal method.

In this work, the LTF calibration method is applied for bi-static GPR scenario. The simplified analytical model developed for bi-static GPR scenario [9] is used as forward model in LTF method. Here we have implemented two approaches for finding measured Green's function. The comparison of Green's function by two approaches is presented. The simplified analytical model developed for two-layered (air-PEC) bi-static GPR [9] is successfully validated with the laboratory measurement results using both the approaches. The corresponding results have been presented.

## II. LTF CALIBRATION METHOD

In this work, bi-static GPR scenario is considered. Two antennas separated by a distance ( $d$ ) are placed in air at a height ( $h_{air}$ ) above ground. The delay caused by antenna and undesired multiple reflections during antenna-medium interaction need to be removed from measured data. The LTF calibration method [6] in frequency domain is given as following:

$$S_{21,k}(\omega) = H_i(\omega) + \frac{H_t(\omega)G_{xx,k}^\dagger(\omega)H_r(\omega)}{1-H_f(\omega)G_{xx,k}^\dagger(\omega)} \quad (1)$$

$$G_{xx,k}^\dagger(\omega) = \frac{\{S_{21,k}(\omega) - H_i(\omega)\}}{H(\omega) + H_f(\omega)\{S_{21,k}(\omega) - H_i(\omega)\}} \quad (2)$$

$H(\omega) = H_t(\omega)H_r(\omega)$ .  $H_t(\omega)$ ,  $H_r(\omega)$  are the transfer functions of transmitting and receiving antenna respectively.  $H_i(\omega)$  gives the transfer function of return loss,  $H_f(\omega)$  represents the feedback loss transfer function.  $G_{xx,k}^\dagger(\omega)$  gives transfer function of the air-subsurface system modelled as a multilayered medium.  $S_{21,k}(\omega)$ , the field that propagates from transmitting antenna to receiving antenna through subsurface, is obtained from laboratory measurements. A copper plate is considered as known object for calibration. The measurements have been taken for multiple heights ( $k=1, 2, 3\dots$ ) of antennas above copper plate. The three unknown functions  $H_i(\omega)$ ,  $H_f(\omega)$  and  $H(\omega)$  are obtained by processing eq. (1) in least squares method [8]. A simplified analytical model (eq.

(3) is used as forward model ( $G_{xx,k}^\uparrow(\omega)$ ) in eq. (1). Once  $H_i(\omega)$ ,  $H_f(\omega)$  and  $H(\omega)$  are known, measured Green's function can be easily obtained from eq. (2).

$$G_{xx} = r_{12} \left( \frac{1}{2\pi i} \right) \left( \frac{1}{\frac{2L_0}{\gamma_0}} \right) e^{-\gamma_0 2L_0} (\cos(\theta_{11})) \quad (3)$$

$$\cos(\theta_{11}) = \left( \frac{h_{air}}{L_0} \right) \quad (4)$$

$$L_0 = \sqrt{(h_{air})^2 + (d/2)^2} \quad (5)$$

Generalized bi-static multilayered GPR media is given in Fig. 1. The bi-static GPR scenario of air-copper plate is given in Fig. 2.

### III. EXPERIMENTAL SETUP

The GPR measurements have been conducted inside GPR lab at NIT Rourkela. Two TEM horn antennas (BBHA 9120A, Schwarzbeck Mess-Elektronik) having dimensions  $24.5 \times 22 \times 14.2$  cm were used. A copper plate is used for calibration. Antenna operating frequency is 800MHz to 5 GHz. But here we have considered for 800 – 2000MHz with 20 MHz spacing. A handheld vector network analyzer (HHVNA- Rhode & Schwartz) is used for recordings. The laboratory setup for bi-static GPR measurement in NIT Rourkela is shown in Fig. 3.

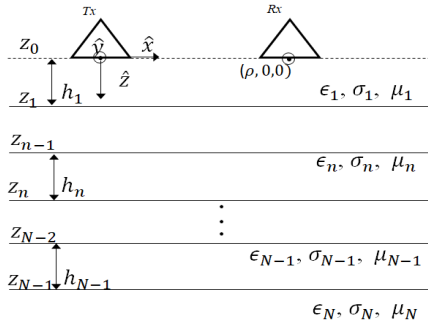


Fig.1. A generalized bi-static multi-layered GPR Scenario

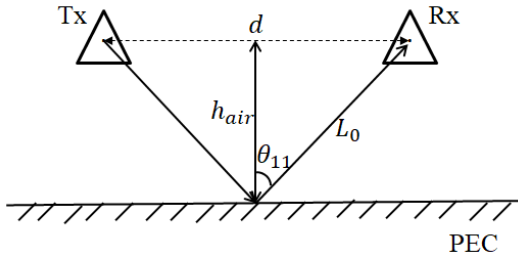


Fig.2. Bi-static GPR Scenario of air-copper plate

### IV. CALIBRATION APPROACHES

To find measured Green's function from measured data, we have implemented two approaches.



Fig. 3. Laboratory Setup of bi-static air-PEC scenario in GPR lab at NIT Rourkela

#### A. Approach-1

The measurements were conducted by placing both the antennas, separated by a distance  $d=30$ cm, at different heights above a copper plate. Both the antennas are aligned in vertical configuration ( $\theta = 0^\circ$ ) as shown in Figure 4(a). The heights (in cm) that considered are  $\{32, 34, 36, 38, 40$  and  $42\}$ . The travelling electromagnetic signal between the transmitting and receiving antennas is assumed to propagate in minimum path. The propagated wave doesn't emit and receive through the main lobe of horn antenna. Both emission and reception occur at some angle which is equivalent to  $\theta_{11}$  which depends on  $h_{air}$  and  $d$ . So the antenna radiation pattern at the received angle is evaluated and incorporated in the calibration procedure. The eq. (2) is modified as follows:

$$G_{xx,k}^\uparrow(\omega) = \frac{\{S_{21,k}(\omega) - H_i(\omega)\}}{\{H(\omega)E^2(\varphi) + H_f(\omega)\{S_{21,k}(\omega) - H_i(\omega)\}} \quad (6)$$

$E(\varphi)$  is the angle dependent radiation pattern at received antenna. This can be evaluated from free-space line of sight (LOS) measurement between the two horn antennas. Both the antennas are placed at fixed distance (here 100cm).  $S_{21}$  has measured when transmitting antenna is placed at  $0^\circ$  angle and received antenna rotates in a desired angle. The magnitude of  $E(\varphi)$  can be evaluated as follows

$$|E(\varphi)| = |\{S_{21}(\omega, \varphi)\} / \{S_{21}(\omega, \varphi = 0)\}| \quad (7)$$

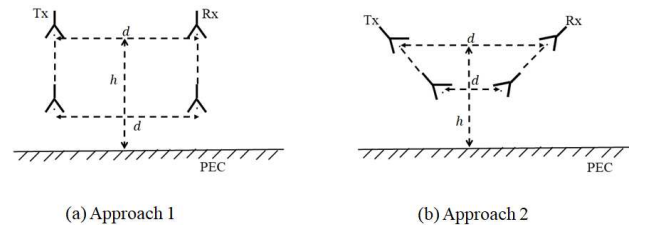


Fig. 4. Calibration approaches

#### B. Approach-2

The measurements were conducted by placing both the antennas, separated by a distance  $d$ , at different heights above a copper plate. Both the antennas are aligned in inclined configuration ( $\theta = 20^\circ$ ) as shown in Figure 4(b). Here the minimum distance between the centers is measured as 23.2cm and the corresponding height is 31.9cm. The angle of

antenna alignment is fixed. Height of the antennas (cm) above copper plate is increased  $\{31.9, 34, 36, 38, 40, 42\}$  and corresponding antenna separation ( $d = 2h \tan \theta$ , where  $\theta$  in degrees) is considered such that the angle of emission and reception is fixed for all the measurements. The measured Green's function is determined by eq. (2).

## V. RESULTS AND DISCUSSION

The measured Green's function is evaluated and compared to that of modelled for both the approaches in frequency domain and time domain. The corresponding results are given in Fig. 5-8. Fig.5 and Fig.6 are results obtained using approach 1 for  $h=36\text{cm}$  and  $38\text{ cm}$  respectively. Fig.7 and Fig.8 are results obtained using approach 2 for  $h=36\text{cm}$  and  $38\text{ cm}$  respectively. These results show that both the calibration approaches are promising for GPR applications. The developed model is successfully validated with laboratory measurements.

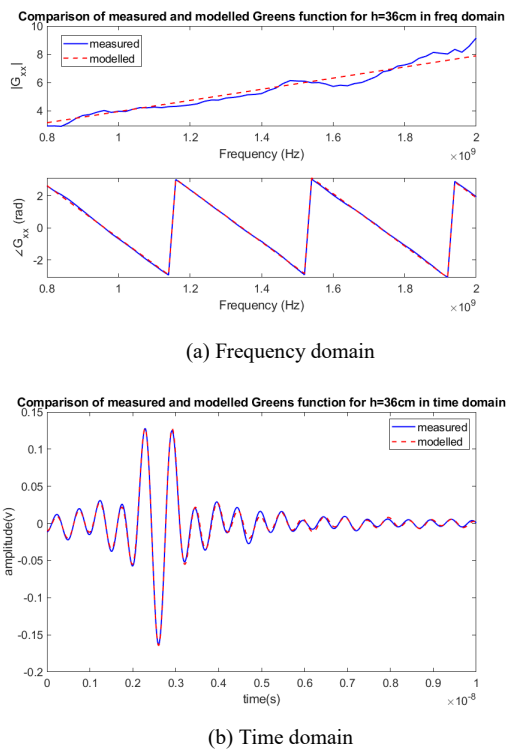


Fig.5. Comparison of measured and modelled Green's function of  $h=36\text{cm}$  for Approach-1.

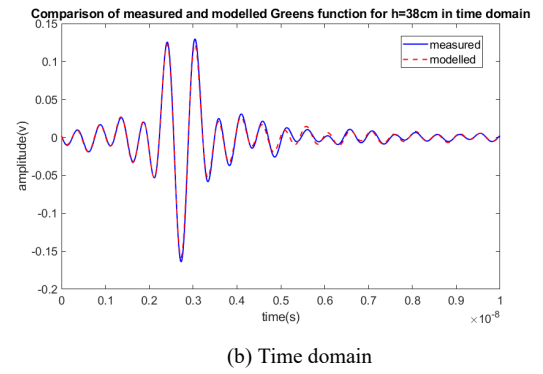
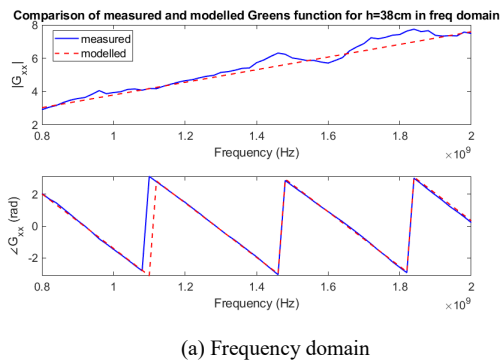


Fig.6. Comparison of measured and modelled Green's function of  $h=38\text{cm}$  for Approach-1

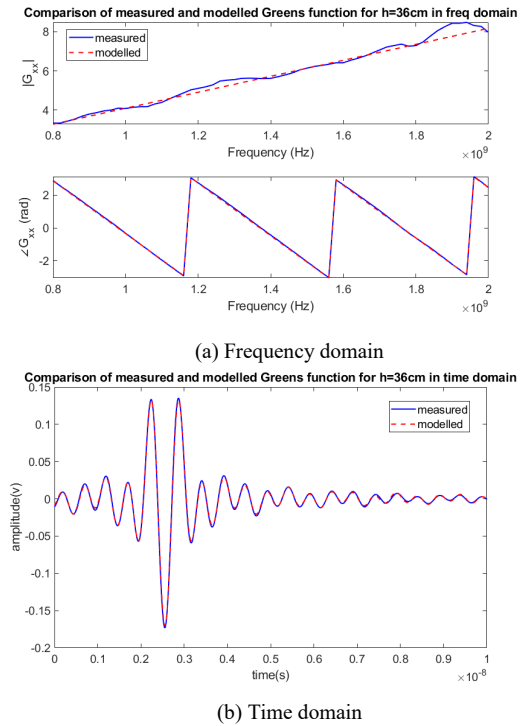
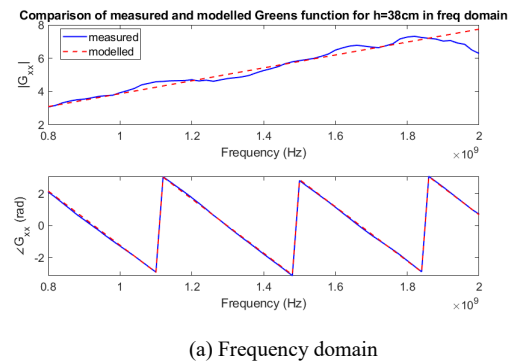
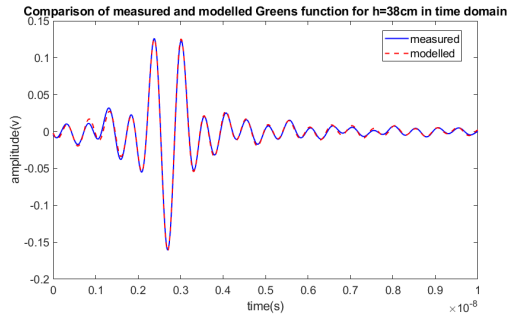


Fig.7. Comparison of measured and modelled Green's function of  $h=36\text{cm}$  for Approach-2.





(b) Time domain

Fig.8. Comparison of measured and modelled Green's function of  $h=38\text{cm}$  for Approach-2.

TABLE 1: Calculation of %RMS error and %cross-correlation coefficient (%CCC) between measured and modelled Green's function for both the approaches

Parameter	Approach-1		Approach-2	
	$h=36\text{cm}$	$h=38\text{cm}$	$h=36\text{cm}$	$h=38\text{cm}$
%RMS error in FD	8.15	9.06	4.94	7.40
%CCC in TD	99.66	99.6	99.89	99.72

We have evaluated the %RMS error and %CCC between measured and modelled Green's function in frequency domain and in time domain respectively. Corresponding results have shown in Table 1. Results show that both the approaches are promising and approach 2 gives better %RMS error and %CCC than approach 1.

## VI. SUMMARY

Accurate GPR measurements depend on accurate calibration techniques. In this work, two different approaches for bi-static GPR have implemented. Measured Green's function is evaluated for both the approaches. The frequency and time domain comparison of measured and modelled responses for antenna heights  $h=36\text{cm}$  and  $38\text{cm}$  for both the

approaches are presented. %RMS error and cross-correlation coefficient (%CCC) have evaluated in each case, given in TABLE 1. These results show that both the calibration approaches are promising for GPR applications. Laboratory measurements successfully validate the developed model in [9].

## ACKNOWLEDGMENT

This research work was supported and sponsored by IMPRINT-II project, SERB INDIA.

## REFERENCES

- [1] W. C. Chew, *Waves and Fields in inhomogeneous media*. IEEE press New York, 1995.
- [2] D.J. Daniels, *Ground penetrating radar*, The Institute of Engineering and Technology, London, U.K, 2007
- [3] M. Nakhkash, Yi Huang, W. Al-Nuaimy and M. T. C. Fang, "An improved calibration technique for free-space measurement of complex permittivity," *IEEE Transactions on Geoscience and Remote Sensing*, vol. 39, no. 2, pp. 453-455, Feb 2001.
- [4] V. A. Mikhnev and P. Vainikainen, "Single-reference near-field calibration procedure for step-frequency ground penetrating radar," *IEEE Transactions on Geoscience and Remote Sensing*, vol. 41, no. 1, pp. 75-80, Jan. 2003.
- [5] E. Korkmaz and P. van Genderen, "Calibration procedures for antenna footprint measurement of stepped frequency CW radar," *Proceedings of the Tenth International Conference on Grounds Penetrating Radar, 2004. GPR 2004.*, 2004, pp. 129-132.
- [6] S. Lambot, E. C. Slob, I. van den Bosch, B. Stockbroeckx and M. Vanclooster, "Modeling of ground-penetrating Radar for accurate characterization of subsurface electric properties," *IEEE Transactions on Geoscience and Remote Sensing*, vol. 42, no. 11, pp. 2555-2568, Nov. 2004.
- [7] S. B. Thomas and L. P. Roy, "A Comparative study on calibration technique for SFCW ground penetrating radar," *2017 International conference on Microelectronic Devices, Circuits and Systems (ICMDCS)*, pp. 1-4, 2017.
- [8] S. Maiti, "Analytical Modelling of Ultra-Wide Band Ground Penetrating Radar for Characterization of Subsurface Media," *PhD dissertation*, NIT Rourkela, India. 2017.
- [9] Maiti, Subrata, Rohit K., Sudipta Maity, and Amitabha Bhattacharya. "A novel bi-static GPR model to simulate two-layered subsurface media." *18th International Conference on Ground Penetrating Radar. Society of Exploration Geophysicists*, 2020.